Application of CFD simulation to validate the BREST-OD-300 primary circuit design

A.V. Tutukin[1], D.A. Afremov[1], K.M. Sergeenko[1], D.V. Fomichev[1]

[1]JSC NIKIET, Moscow, Russian Federation

E-mail contact of main author: a.tutukin@nikiet.ru

Abstract. The paper presents a brief overview of modeling the lead coolant flow in the BREST-OD-300 reactor facility primary circuit during rated operation of the reactor, as well as the steady-state conditions of the coolant flow with one of the main circulation pumps (MCP) out of operation. Information has been obtained on the flow rate distribution by parallel lines, the positions of free levels and the heat/mass transport processes in the BREST-OD-300 components. It is possible to determine experimentally hydraulic characteristics only for the core elements on their full-scale mockups. The rest of the primary circuit components require a computational study to be supported by experiments on fragment models. A 3D nature of the flow in the facility's primary circuit requires the use of computational fluid dynamics (CFD) tools.

The CFD model includes the BREST-OD-300 primary circuit. Porous approximation was applied to simulate the flow in the reactor core and the steam generators (SG). The hydraulic parameters of porous regions have been determined both experimentally and by preliminary CFD calculations. The experience of the CFD code verification was taken into account for the liquid metal coolant flow calculation.

The results of modeling operating conditions with different numbers of loops in operation are presented. The key primary circuit parameters adopted in the reactor facility design have been confirmed. Information on the spatial distribution of the coolant's thermal parameters is useful in the formulation of requirements to the arrangement of the reactor instrumentation and control system detectors.

Key words: BREST-OD-300, primary circuit, CFD, RANS

1. Introduction

The BREST-OD-300 lead cooled reactor facility has an integral layout of the key components and is developed in a two-circuit configuration. Once-through steam generators (SG), main circulation pumps (MCP) and primary circuit technological equipment are installed immediately inside the reactor unit's concrete vessel [1] - [4].

Presently, computational fluid dynamics (CFD) codes used extensively to address practical engineering problems. Use of CFD codes combined with experimental studies allows to reduce the development cost and time for new designs. This becomes possible thanks to a reduction in the number of expensive experiments and through optimization of designs at the development stage based on data obtained from an analysis into the distribution of physical quantities obtained in a CFD calculation.

One of the key practical tasks involved in the development of the BREST-OD-300 reactor facility and requiring the use of CFD simulation is estimation of thermal-hydraulic characteristics of the primary circuit.

A commercial CFD code ANSYS CFX 17.0 was used in simulation [5]. The porous approximation was applied to simulate the flow in the reactor core, steam generators (SG), coolant filters and mass exchangers while the rest part of the primary circuit was simulated in RANS approximation. The major applied objectives for the study were:

- determination the elevations of the coolant free levels;
- determination the hydraulic characteristics of the primary circuit used to close the BREST-OD-300 primary circuit models for codes in lumped parameters (system codes);
- estimation the non-uniformity in the coolant velocity and temperature distribution within the primary circuit during rated operation of the reactor and in conditions when one of the main circulation pumps (MCP) is out of operation.

2. Problem definition

2.1. Mathematical model

The coolant is represented by a Newtonian fluid with temperature-dependent thermal properties [6]. In a RANS approximation, the coolant flow is described by a system of equations [7]:

$$\frac{\partial \rho}{\partial t} + \frac{\partial}{\partial x_i}(\rho u_i) = 0, \ i = 1..3, \tag{1}$$

$$\frac{\partial}{\partial t}(\rho u_i) + \frac{\partial}{\partial x_j}(\rho u_i u_j) = -\frac{\partial p}{\partial x_i} + \frac{\partial}{\partial x_j}(\tau_{ij}), \tag{2}$$

where u_i are the velocity components, ρ is density, p is pressure, and dτ_{ij} are components of the shear stress tensor:

$$\tau_{ij} = (\mu + \mu_t) \cdot \left(\frac{\partial u_j}{\partial x_i} + \frac{\partial u_i}{\partial x_j} - \frac{2}{3} \frac{\partial u_k}{\partial x_k} \delta_{ij} \right), \tag{3}$$

where δ_{ij} is a single matrix, and μ and μ_t are the flow molecular and turbulent viscosities respectively.

For the heat and mass transport calculation, an averaged energy equation as follows is added to the system of turbulent flow equations:

$$\frac{\partial}{\partial t}\left[\rho \left(e + \frac{1}{2} u_i u_i \right) \right] + \frac{\partial}{\partial x_j}\left[\rho u_j \left(h + \frac{1}{2} u_i u_i \right) \right] = \frac{\partial}{\partial x_j}\left(\left(\lambda + \frac{c_p \mu_t}{\mathrm{Pr}_t} \right) \frac{\partial T}{\partial x_j} + u_i \tau_{ij} \right), \tag{4}$$

where λ is the coolant heat conduction coefficient, e is the internal energy, h is the specific enthalpy and Pr_t is the turbulent Prandtl number.

The computational model is limited by the BREST-OD-300 primary circuit volume occupied by the lead coolant. The computational domain is limited by the coolant pressure level plane from above and by the reactor cavity bottom from below. The free level elevation values were adopted in the design of normal operation. The model includes regions of porous domains (reactor core, steam generator modules, coolant filters, mass exchangers, sealing units) and RANS domain for simulation of the rest part of the primary circuit. Fig. 1 shows the arrangement of the BREST-OD-300 primary circuit components inside the reactor vessel. Highlighted in Fig. 1b is the arrangement of the reactor facility’s structural components simulated in a porous-body approximation, and the coolant-occupied primary circuit volume is shown by semi-transparent geometrical bodies.

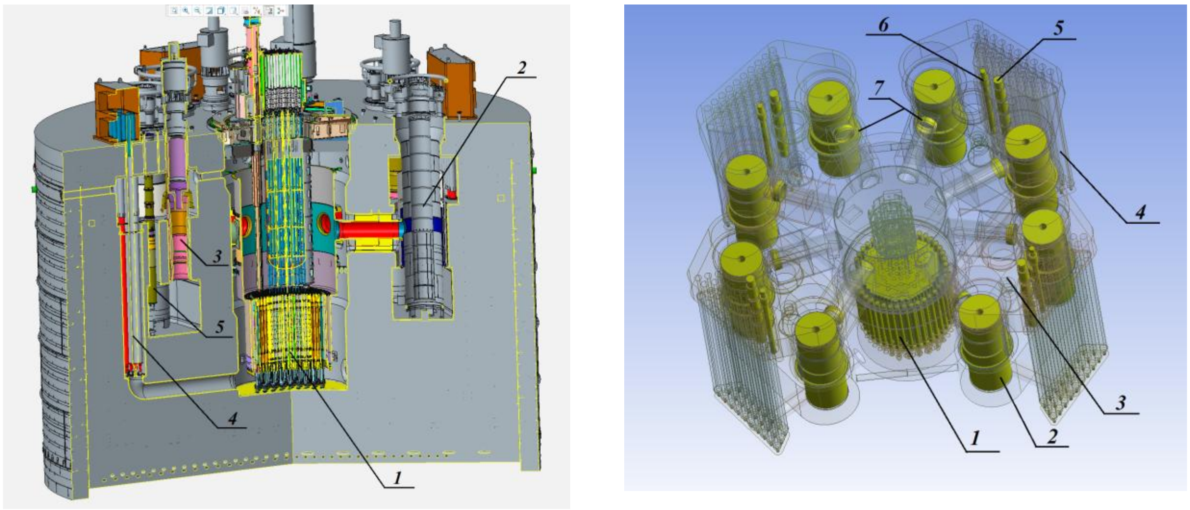

a) b)

a) Primary circuit equipment composition; b) Porous domains locations in the primary circuit model
1 - core; 2 - steam generator; 3- MCP; 4 - heat exchanger; 5 - filter; 6 - mass exchanger; 7 - sealing.
FIG. 1. Primary circuit model

The general equation of transport in a porous medium has the form

$$\frac{\partial}{\partial t}(\gamma\rho\Phi) + \nabla\cdot\left(\rho\boldsymbol{K}\cdot\vec{U}\Phi\right) - \nabla\cdot(D\boldsymbol{K}\cdot\nabla\Phi) = \gamma S, \qquad (5)$$

where Φ is the sought-after function, γ is the bulk porosity, $\boldsymbol{K}=\{K^{ij}\}$ is the symmetrical second-rank tensor, $\vec{U}$ is the flow velocity (that is, calculated for the effective cross-section), D is the diffusion coefficient, S is the source function used to allow for the fluid interaction with the solid-body components in the volume occupied by the porous body. In this study the isotropic tensor $\boldsymbol{K}$ is used, which means that the condition $K^{ij} = \gamma\delta^{ij}$ should be fulfilled, where δ^{ij} is the Kronecker symbol.

The equations of the momentum continuity and conservation in a porous medium have the form:

$$\frac{\partial}{\partial t}(\gamma\rho) + \nabla\cdot\left(\rho\boldsymbol{K}\cdot\vec{U}\right) = 0 \qquad (6)$$

$$\frac{\partial}{\partial t}(\gamma\rho\vec{U}) + \nabla\cdot\left(\rho(\boldsymbol{K}\cdot\vec{U})\otimes\vec{U}\right) - \nabla\cdot\left(\mu_{eff}\boldsymbol{K}\cdot\left(\nabla\vec{U} + \left(\nabla\vec{U}\right)^{T} - \frac{2}{3}\delta\nabla\vec{U}\right)\right) = \gamma S_M - \gamma\nabla p, \qquad (7)$$

where μ_{eff} is the effective dynamic viscosity coefficient, and S_M is the source function.

The equation of heat transport in a porous medium has the form:

$$\frac{\partial}{\partial t}(\gamma\rho h) + \nabla\cdot\left(\rho\boldsymbol{K}\cdot\vec{U}h\right) - \nabla\cdot(D_e\boldsymbol{K}\cdot\nabla h) = S^{h}, \qquad (8)$$

where h is the total specific enthalpy, D_e is the effective thermal diffusion coefficient, and S^h is the source function.

The hydraulic parameters of porous domains were found both experimentally (core elements, coolant filter, mass exchanger) and based on preliminary CFD calculations (steam generators, sealing units).

A two-parameter standard k - ε turbulence model with a scalable wall function was used to describe the turbulent transport processes [8].

2.2. Boundary conditions

Simulation was based on numerical solution of Reynolds-averaged Navier-Stokes equations. Only steady states were considered. The MCP operation was simulated using inlet type and outlet type boundary conditions. To model the reactor operation with one of the MCP out of operation, the flow rate through the inactive pump was given in accordance with the hydraulic characteristic found experimentally. Boundary conditions of the wall type are given for the surfaces matching the positions of the coolant free levels. Boundary conditions of the wall type are given for the rest of the computational domain's outer boundary surfaces as well. The power of the core heat sources and the heat sinks in the steam generators, and the temperature distribution by the heat-transfer surfaces of the cooldown heat exchanger channels, were given in accordance with the design documentation data. The circuit metal structures are not included in the circuit CFD model. Therefore the heat transfer through the separation steel surfaces between the hot coolant flow from the reactor core to the SG and the cold flow on descending part of the circuit hydraulic path was taken into account by means of additional heat surface sources, defined on the corresponding wall-type boundaries. No heat sink into the inactive SG was assumed for the case with one MCP out of operation. The overall view of the computational domain with respective boundary conditions is shown in Fig. 2.

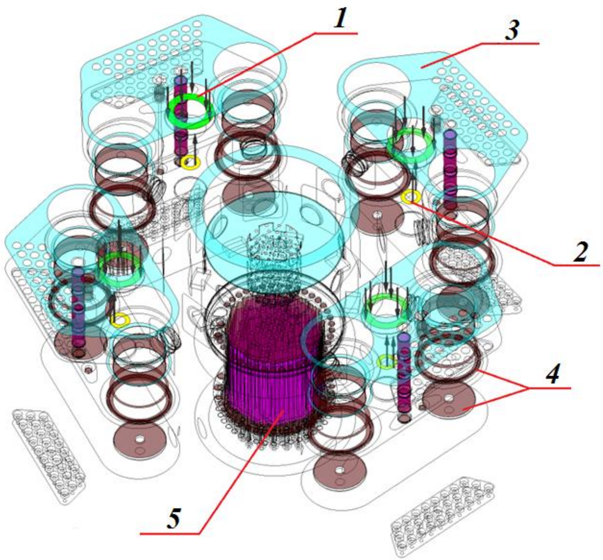

1 - inlet; 2 - outlet; 3- free levels; 4 - interfaces; 5 - interfaces inside core model.
FIG. 2. Boundary locations (4 MCP in operation)

2.3. Discretization of the computational domain

Calculations were performed on a non-structured grid containing tetrahedral, hexagonal and prismatic reference volumes. The finite volume grid of the BREST-OD-300 primary circuit hydraulic path was developed using the ANSYS Meshing 17.0 and ANSYS ICEM CFD 17.0 grid construction packages. The total number of reference volumes in the computational model was about 130 million. The lead-occupied volume is simulated by approximately 120 million reference volumes, while porous domains account for the rest. The minimum number of reference volumes in the primary circuit hydraulic path's slit channels is 5. The maximum dimensionless distance y^+ for the wall-adjacent reference volume center does not exceed 150. The grid convergence was examined only for some of the primary circuit lengths at the computational model development stage. For the discretization the systems of energy and momentum conservation equations the ANSYS CFX High Resolution Scheme is used. All calculations were performed with double precision solver. The stopping criteria for the calculation are: the value of RMS residuals for the continuity and energy conservation equations is 10^{-6} and the RMS residuals value of momentum conservation equation is 10^{-4}. The global imbalances for each solved equation does not exceed $2{\cdot}10^{-5}$.

3. Results

3.1. Hydraulic characteristics of the reactor core elements

The parameters needed to find the closing relations of the porous-body models matching the core's structural elements were obtained based on results of an experimental study conducted at JSC NIKET and confirmed by results of cross-verification calculations based on ANSYS FLUENT 17.0 and LOGOS, a Russian CFD code developed by VNIIEF [9]. Fig. 3 shows the results of comparing the hydraulic characteristics of the fuel assembly head and tail found both experimentally and as part of the FLUENT and LOGOS simulations. The results are presented in a dimensionless form, and the maximum pressure drop difference between the calculation results and the experiment does not exceed 7% .

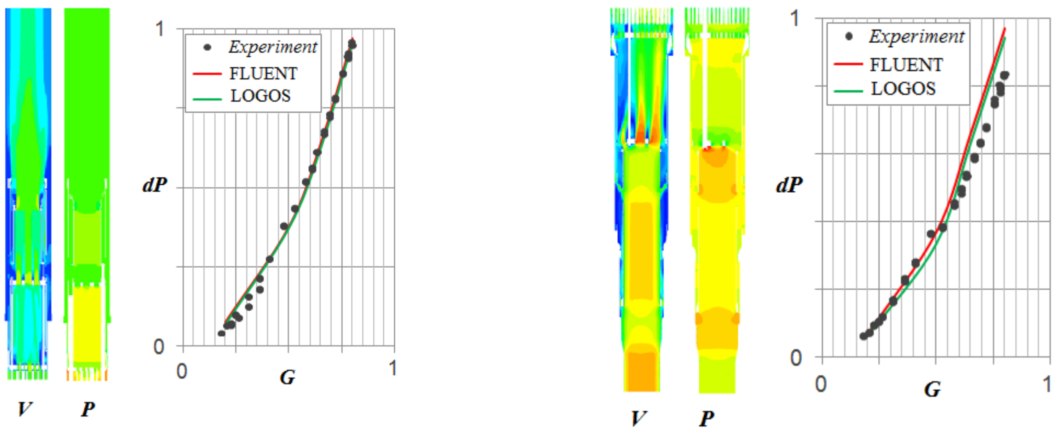

a) *b)*

a) fuel assembly head; b) fuel assembly tail

FIG. 3. Characteristics of the core structural elements

3.2. Hydraulic characteristics of the steam generator

The parameters needed to find the closing relations for the steam generator porous-body models were obtained based on CFD calculations in the STAR-CCM+ code [10]. The experience of the CFD code verification was taken into account in the computational model construction for the liquid metal coolant flow calculation [11]. Fig. 4 presents a computational velocity field in a vertical plane passing through the SG axis. The velocity is given in dimensionless units. It can be seen from Fig. 4 that the velocity field is arranged uniformly. Local flow perturbations are expectedly observed near perforation holes and spacers. The CFD data was compared against the procedure [12]. The CFD-calculated hydraulic resistance coefficient proved to be approximately 10% as low as the estimate obtained with the use of the procedure [12]. Given the fact that most engineering procedures are conservative relative to the parameters being determined, this divergence in the calculated SG hydraulic resistance coefficients has been assumed to be acceptable.

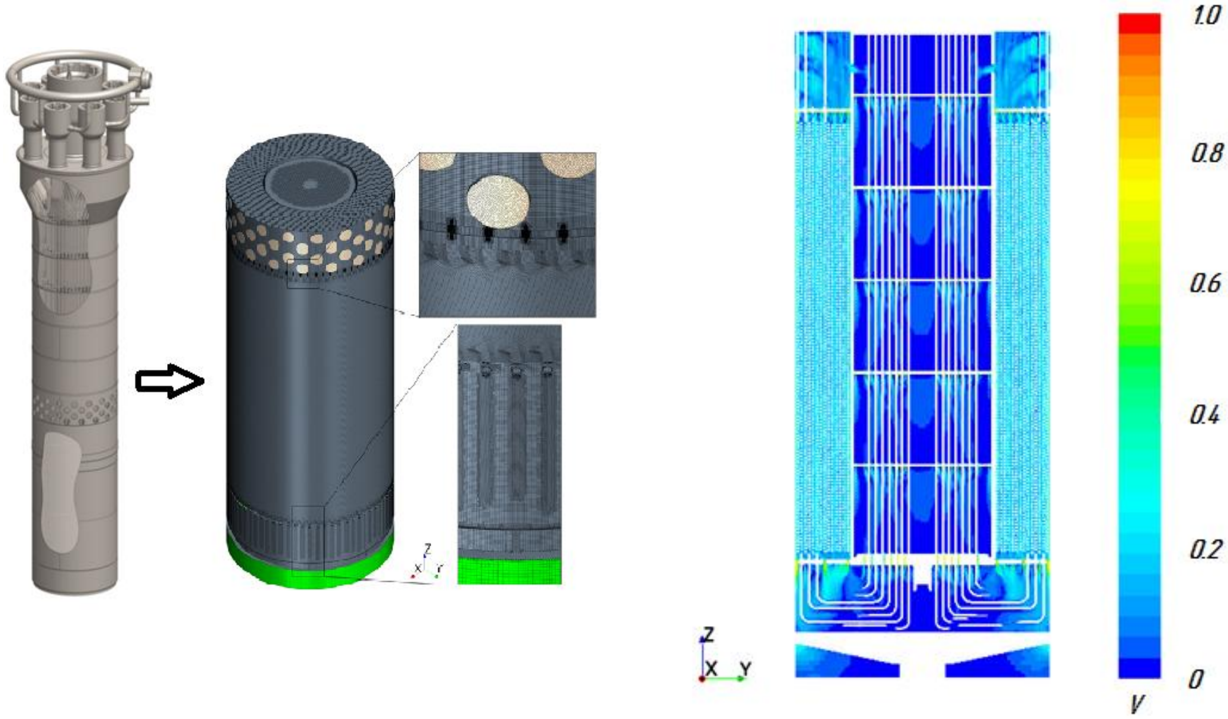

a) *b)*

a) steam generator model; b) dimensionless velocity distribution

FIG. 4. SG characteristics

3.3. Thermal-hydraulic characteristics of the primary circuit

One of the key tasks was to determine elevations of the coolant free levels within the primary circuit. The coolant flow was modeled in a single-phase approximation. The positions of the coolant free levels were calculated indirectly against the initial level of the primary circuit filling, with regard to the difference in the average pressures on the boundaries that matched the steady-state free level elevations during partial or full power operation of the reactor. Figs. 5 and 6 show dimensionless steady-state distributions of the lead velocity and temperature in representative primary circuit sections during the reactor rated operation and with one of the MCP being inactive. The key parameters of the primary circuit have been confirmed for the rated operation, including the positions of the coolant free levels.

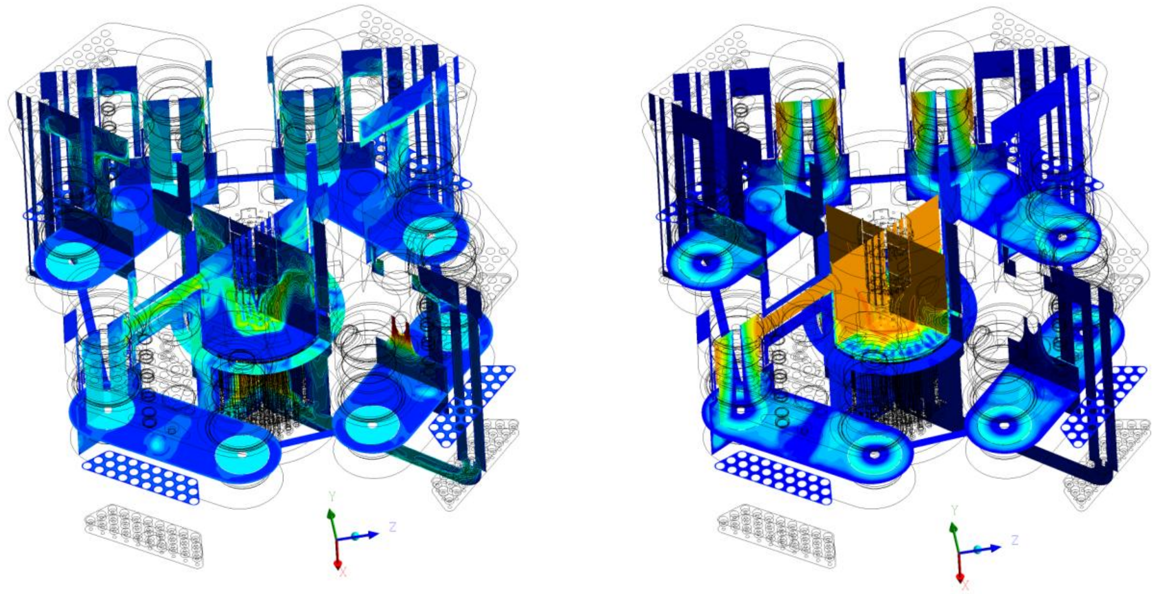

a) *b)*

a) dimensionless velocity distribution; b) dimensionless temperature distribution

FIG. 5. Primary circuit characteristics with 4 MCPs in operation

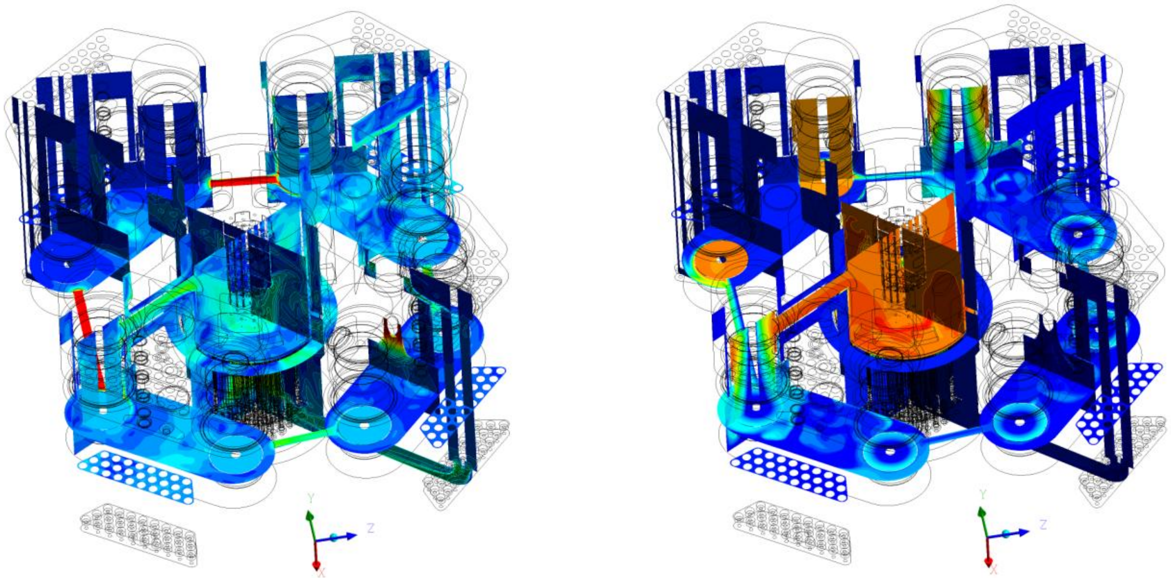

a) *b)*

a) dimensionless velocity distribution; b) dimensionless temperature distribution

FIG. 6.Primary circuit characteristics with 3 MCPs in operation

4. Conclusion

A distinctive feature of the BREST-OD-300 reactor facility is the configuration of the primary circuit that the lumped-parameter code approximation could have a high calculation error, especially in the local areas with high physical values gradients. Given the specific equipment arrangement in the BREST-OD-300 vessel, experimental validation of thermal-hydraulic characteristics on full-scale mockups becomes possible only for some of the primary circuit components, such as the core elements. For other elements of the primary circuit experimental studies are possible on small- and medium-scale models. To validate the thermal-hydraulic characteristics of the BREST-OD-300 steam generator and the primary circuit, CFD simulation methods in a RANS approximation were used.

The results of the study have confirmed the basic parameters of the primary circuit adopted in the reactor facility design, and information has been obtained concerning the flow distribution by parallel hydraulic paths, the positions of free coolant levels and the heat/mass transport processes in the lead-occupied primary circuit volume. Information on the spatial distribution of the coolant's thermal parameters is useful as well for the formulation of requirements to the arrangement of the instrumentation and control system detectors.

5. References

[1] Yu.G. Dragunov, V.V. Lemekhov, A.V. Moiseev, V.S. Smirnov. Lead Cooled Fast – Neutron Reactor (BREST). INPRO Dialog-Forum, IAEA HQ, Vienna, Austria, May 26- 29 2015, p 32.

[2] Yu.G. Dragunov, V.V. Lemekhov., V.S. Smirnov, N.G. Chernetsov. Technical solutions and development stages for the BREST-OD-300 reactor unit. – «Atomic Energy» 2012, Vol. 113, No. 1, pp. 58-64.

[3] Yu.G. Dragunov, V.V. Lemekhov., V.S. Smirnov. Fast Neutron Reactor with Lead Coolant (BREST). ISTC NIKIET-2014, JSC NIKIET, Moscow, Russia, 2014. – Vol.1, pp. 94-102.

[4] Yu.G. Dragunov, V.V. Lemekhov., A.V. Moiseev, V.S. Smirnov at all. Detailed design of the BREST-OD-300 reactor facility: development stages and justification. ISTC NIKIET-2016, JSC NIKIET, Moscow, Russia, 2016.,Vol.1, pp.21-30.

[5] ANSYS CFX Solver Theory Guide. Release 17.0. ANSYS Inc. 2015.

[6] P.L. Kirillov, V.P. Bobkov, A.V. Zhukov, Yu.S. Yuryev. Reference Book on Thermal-Hydraulic Calculations in Nuclear Power. Volume 1. Thermal-Hydraulic Processes in Nuclear Power. Moscow: IzdAT, 2010 (in Russian).

[7] Tannehill J.C., Anderson D.A., Pletcher R.H. Computational Fluid Mechanics and Heat Transfer: In 2 vol. *Vol*. 2, 1990, Moscow, Mir Publ., 392 p. (in Russian).

[8] Launder B.E., Spalding D.B. The Numerical Computation of Turbulent Flows. Comp. Meth. In Appl. Mech. And Eng., 1974, p. 269-289.

[9] A.S. Kozelkov, Yu.N. Deryugin, D.K. Zelenskiy, V.A. Glazunov, A.A. Golubev, O.V. Denisova, S.V. Lashkin, R.N. Zhuchkov, N.V. Tarasova, M.A. Sizova. LOGOS Multifunctional Software Package for the Calculation of Fluid Dynamics and Heat/Mass Transport Problems on Multiprocessor Computers: Base Technologies and Algorithms//Supercomputations and Mathematical Modeling: Proceedings of the 12th International Workshop. Sarov, 11-15 October 2010. PP. 215-230 (in Russian).

[10] User Guide. Star-CCM+ Version 10.02 – CD-adapco, 2015.

[11] N.V. Meleshkin, O.Ye. Vlasova, A.A. Deulin, A.S. Krivonos, N.V. Krivonos, O.L. Krutyakova, O.O. Oskolkova, Yu.A. Tsybereva, D.V. Fomichev. Verification of the LOGOS Software Package to Model Liquid Metal Coolant Flows in Fast Reactor Components // Innovations in Nuclear Power: Book of Reports for the Conference of Young Specialists (25-26 November 2015, Moscow). – Moscow: JSC NIKIET Publ., 2015. PP. 261-272. (in Russian).

[12] Thermal and Hydraulic Design of the NPP Heat-Exchange Equipment. RD 24.035.05-89, NPO TsKTI, Leningrad, 1991 *(*in Russian).